[1)]This approach has a rigorous basis for the case of longitudinal sound[2,3] but does not take into account the transformation of a transverse sound wave into an electromagnetic wave. This transformation leads to additional sound absorption owing to the evolution of Joule heat, and this substantially alters the frequency dependence of the absorption coefficient when $\lambda \approx \delta(\omega)$, where $\delta(\omega)$ is the skin penetration depth for electromagnetic wave of the sound frequency ω. The sound absorption coefficient resulting from this mechanism is of the same order as the absorption coefficient due to the deformation interaction.[4] The formulas for the acoustoelectric effect presented below are exact for longitudinal sound and are correct in order of magnitude for transverse sound [when $\lambda \neq \delta(\omega)$]. Strictly speaking, the formulas derived here describe the acoustoelectric effect for $ql \gg 1$, which is due to the deformation interaction.

[2)]We are indebted to P. E. Zil'berman for calling our attention to this fact.

[3)]The hermiticity of $\hat{W}$ for the case of electron scattering by impurities and phonons has been directly verified (see Ref. 11). The problem of the hermiticity of W and the possible consequences of its violation has not been thoroughly studied.

[4)]We note that if the sound does not propagate along one of the selected crystallographic directions, $\mathbf{q}$ will not be parallel to $\mathbf{s}_{\mathbf{q}}$, while the energy flux Φ will be parallel to $\mathbf{s}_{\mathbf{q}}$.

[5)]A crystal symmetry plane is always a symmetry plane of the Fermi surface, but such a plane need not intersect the Fermi surface. Not every symmetry plane of the gap in the Fermi surface is a crystal symmetry plane.

[1]R. H. Parmenter, Phys. Rev. **89**, 990 (1953); V. L. Gurevich, Fiz. Tekhn. Poluprovodn. **2**, 1557 (1968) [Sov. Phys. Semicond. **2**, 1299 (1968)].

[2]A. I. Akhiezer, M. I. Kaganov, and G. Ya. Lyubarskiĭ, Zh. Eksp. Teor. Fiz. **32**, 837 (1957) [Sov. Phys. JETP **5**, 685 (1957)]; A. B. Pippard, Philos. Mag. **46**, 1104 (1955).

[3]L. E. Gurevich, Zh. Eksp. Teor. Fiz. **16**, 416 (1946); Izv. Akad. Nauk SSSR Ser. Fiz. **21**, 112 (1957).

[4]Eugene I. Blount, Phys. Rev. **114**, 418 (1959); V. M. Kontorovich, Zh. Eksp. Teor. Fiz. **45**, 1638 (1963) [Sov. Phys. JETP **18**, 1125 (1964)].

[5]F. Bloch, Z. Phys. **59**, 208 (1930).

[6]N. V. Zavaritskiĭ, M. I. Kaganov, and Sh. T. Mevlyut, Pis'ma v Zh. Eksp. Teor. Fiz. **28**, 223 (1978) [JETP Lett. **28**, 205 (1978)].

[7]I. M. Lifshitz, M. Ya. Azbel' and M. I. Kaganov, Zh. Eksp. Teor. Fiz. **31**, 63 (1956) [Sov. Phys. JETP **4**, 41 (1957)].

[8]I. M. Lifshitz, M. Ya. Azbel' and M. I. Kaganov, Elektronnaya teoriya metallov (Electron theory of metals), Nauka, 1971 (Engl. transl. Consultants Bureau, N. Y., 1973).

[9]John M. Ziman, Electrons and phonons; the theory of transport phenomena in metals, Clarendon Press, Oxford, 1960 (Cited in Russian translation).

[10]M. Ya. Azbel' and É. A. Kaner, Zh. Eksp. Teor. Fiz. **32**, 896 (1957) [Sov. Phys. JETP **5**, 730 (1957)].

[11]I. M. Lifshitz and M. I. Kaganov, Usp. Fiz. Nauk **87**, 389 (1965) [Sov. Phys. Usp. **8**, 805 (1966)].

[12]N. V. Zavaritskiĭ, Zh. Eksp. Teor. Fiz. **75**, 1873 (1978) [Sov. Phys. JETP **48**, 942 (1978)].

[13]Gabriel Weinreich, Phys. Rev. **107**, 317 (1957).

Translated by E. Brunner

Partial composition of a dense electron-hole system and exciton-plasma transition in uniaxially stressed silicon

V. D. Kulakovskiĭ, I. V. Kukushkin, and V. B. Timofeev

Institute of Solid State Physics, USSR Academy of Sciences

(Submitted 21 August 1979)
Zh. Eksp. Teor. Fiz. **78**, 381–394 (January 1980)

A high-density nonequilibrium electron-hole system is investigated in silicon crystals that are elastically deformed along the ⟨100⟩ axis, at temperatures $T \lesssim 20$ K. The two-phase gas + electron-hole liquid region is determined, and the critical temperature of the phase transition is estimated at $T_c = (14 \mp 1.5)$ K. Investigations of the photoconductivity and of the recombination radiation spectra, as well as of the kinetics of the spectra under pulsed excitation, are used to analyze the partial composition of the gas phase in a wide range of excitation densities, up to densities corresponding to the dimensionless parameter $r_s \sim 1.5$. It is established that when the density is increased to $r_s = 2.7 \mp 0.3$ and at $T = 12.5$ K the gas phase consists predominantly of excitons and excitonic molecules. An investigation of the transformation of a gas of excitons (biexcitons) into an electron-hole plasma at $T \gtrsim T_c$ has shown that the excitonic states disintegrate at densities corresponding to $r_s^* = 2.5$–2. The obtained value of r_s^* differs noticeably from the critical density estimated from Mott's criterion for an exciton-plasma transition, and comes close to the value of r_s^* calculated in the approximation of dielectric screening of the excitons.

PACS numbers: 71.35. + z, 71.45. − d, 64.60. − i, 72.40. + w

1. INTRODUCTION

An exciton gas of sufficiently high density can condense in semiconductors at low temperatures into an electron-hole liquid (EHL).[1,2] This condensation of the excitons is a first-order phase transition. The region of the coexistence of the gas and liquid phases in a nonequilibrium electron-hole (e-h) system is determined by a phase diagram usually plotted with the density and temperature as coordinates. The gas–EHL phase diagrams were investigated most thoroughly in the indirect semiconductors germanium[3,4] and silicon.[5,6] In these semiconductors, the binding energy in the liquid, relative to the excitonic term, turns out to be quite large (~0.4 Ry in Ge and 0.6 Ry in Si, where Ry the excitonic Rydberg), this being attributed to the strong degeneracy of the electron and hole bands.[7] The lifetimes in the liquid and gas phases in Ge and Si exceed the characteristic thermalization times. Therefore the condensation into drops of metallic EHL in these crystals

0038-5646/80/010191-08$02.40

takes place in quasi-equilibrium conditions and in the low-temperature part of the phase diagram it sets in at relatively low average exciton densities $\bar{n}$, corresponding to the dimensionless parameter $r_s \equiv (3/4\pi\bar{n})^{1/3} a_B^{-1} \gg 1$ (a_B is the Bohr radius), when the exciton gas constitutes a weakly interacting Boltzmann gas.

Up to now, the most thoroughly investigated were the properties of the liquid phase. It was established by experiment that it is well described by the properties of the two-component Fermi liquid. As to the properties of the gas phase along the gas–EHL phase boundary, a number of fundamental questions still remain unanswered. One of them is connected with the multicomponent composition of the e-h gas. The point is that besides the free carriers and excitons, this gas can contain also more complicated free multiparticle complexes—excitonic molecules and trions (bound states of an exciton with an electron or a hole[8]), whose stability follows from variational calculations. The question of the partial composition of the gas phase along the gas–EHL equilibrium line still remains open. In Ge and Si at low temperatures, $T \ll T_c$, the gas phase is dielectric and consists mainly of excitons, this being due to the low binding energy of the biexcitons and of the trions in comparison with the EHL. The unique situation, wherein the densities of the excitons and of the excitonic molecules are of the same order, has apparently been observed so far only in silicon compressed along the ⟨100⟩ axis, where the EHL binding energy is negligibly small, and at low temperatures. With increasing temperature the density of the gas phase increases along the boundary of the equilibrium of the gas with the EHL. Effects of thermal ionization and screening of the Coulomb interaction then come into play. Two criteria are discussed in the literature for the critical density $n_c(r_s^c)$ at which the ionization catastrophe of the exciton sets in and the dielectric gas of the excitons is transformed into an e-h plasma [the exciton-plasma (EP) transition]. One of the criteria (frequently called in the literature the Mott criterion), based on a numerical solution of the two-particle Schrödinger equation with a statically screened Coulomb potential $V(r) = e^2 \exp(-r/r_0)/\varkappa r$, indicates that the binding energy of the exciton vanishes when[9]

$$r_0(\bar{n}) \approx 0.84 a_B, \qquad (1)$$

where $r_0(n)$ is the static screening radius.[1)] For a model semiconductor with straight bands and with isotropic and equal effective masses $m_e = m_h$, according to this plasma-screening criterion the EP transition at $T = 0$ K sets in at critical densities corresponding to $r_s^{cp} \approx 6.8$.[9] Within the framework of the other approach, the critical density $n_c(r_s^{cd})$ is estimated, on the basis of the dielectric screening of the Coulomb interaction,[11] from the "collapse" of the energy gap in the spectrum of the single-particle collective excitations in the high-density exciton system. According to this approach, the excitons remain stable at substantially higher density, up to $r_s^{cd} \approx 1.8$, i.e., so long as the wave functions of the excitons do not overlap strongly.[11] We note that in the case of an impurity system we have $r_s^{cp} \approx r_s^{cd} \approx 1.7$.[12,13] It still remains unclear which of the criteria corresponds to the experimental data, and whether the EP transition has the character of a phase transition[14] and exhibits singularities along the gas-liquid phase boundary.[15,16]

For experimental investigations of the above-mentioned group of problems, we have chosen crystals of silicon Si(1–2) uniaxially deformed along the ⟨100⟩ direction (the numbers 2 and 1 denote the multiplicity of the degeneracy of the electron and hole bands). The choice of this subject was governed by the following. Because of the strong lifting of the band degeneracy in Si(1–2), the liquid phase turns out to be much less stable compared with the undeformed crystals Si(2–6). This shifts the gas–EHL phase boundary by more than one order of magnitude towards higher densities. It turned out that in such a dense e-h gas at low temperatures the concentrations of the excitons and of the excitonic molecules are of the same order. This has made it possible to use the radiative-recombination spectra and the photoconductivity to trace the partial composition of the gas phase (excitons, excitonic molecules, free electrons and holes) up to densities corresponding to $r_s \approx 2.5$. We investigated also the thermodynamic properties of the EHL at $T \lesssim 10$ K and analyzed the problem of the EP transition.

2. EXPERIMENTAL PROCEDURE AND CRYSTALS

We used single crystals of pure silicon with a concentration of the residual electrically active impurities (mostly boron) $N \lesssim 10^{13}$ cm^{-3}. The samples were rectangular parallelepipeds with linear dimensions $1 \times 3 \times 10$ mm. The deformation was along the largest linear dimension of the samples. The procedure used for the uniform uniaxial elastic compression of the crystals is described in Ref. 17. Prior to each placement in the cryostat, the samples were etched in a mixture of hydrofluoric and nitric acids (1:3). The investigations were made with the samples placed either in liquid helium ($T \lesssim 4.2$ K) or in its vapor for measurements at higher temperatures. At $T > 5$ K the temperature was stabilized accurate to 0.1 K.

Under the experimental conditions, the homogeneity of the deformation was high enough, judging from the emission line shapes of the free exciton and of the exciton-impurity complex. Thus, at a spectral resolution 0.25 eV and at bulk excitation we noted no inhomogeneous broadening of the TA component of the exciton line (which is narrower than the TO-LO component), nor of the emission lines of the exciton-impurity complexes, up to uniaxial pressure 7–8 kbar.

The nonequilibrium carriers were excited by sources of both pulsed and continuous excitations. For pulsed pumping we used a copper-vapor laser (power and duration of single pulse 5 kW and 10 nsec, pulse repetition frequency 15 kHz, lasing wavelength 5105 Å). This laser made possible pulsed excitation of nonequilibrium e-h pairs near the sample surface, with density up to $(5–7) \times 10^{17}$ cm^{-3}. The source of the continuous bulk excitation was a neodymium laser with aluminum-yttrium garnet (lasing wavelength 1.064 μm, power 5 W). This source ensured a stationary e-h pair concentration up

to 5×10^{15} cm^{-3} in Si(1–2) at pressures 6–7 kbar. An argon laser of ~1 W power was used for continuous surface excitation.

The spectral instrument was a double monochromator with dispersion 10 Å/mm. The radiation receiver was a cooled photomultiplier with S-1 cathode, operating in the photon-counting regime. In the case of pulsed excitation, we used a registration system working in the strobe-integration regime. The employed system of pulsed registration made it possible to measure the kinetics of the emission spectrum as well as the photoconductivity, with a time resolution 0.1–10 μsec. When a constant source was used, its radiation was modulated at a frequency 60 Hz and at a pulse duration 0.2 sec. This quasi-continuous regime ensured minimal heating of the sample. The electron temperature was monitored against the width of the exciton-emission line.

For the measurments of the photoconductivity we soldered to the center of the sample two indium contacts separated by 1–1.5 mm. The contact dimension was ~0.4 mm. After breakdown with a high-frequency discharge ($V\sim80$ kV, $f\sim50$ kHz), the contacts became symmetrical down to helium temperatures. The current-voltage characteristics of such contacts, measured under conditions of weak illumination ($n_{e,h}\lesssim10^{10}$ cm^{-3}) at helium temperatures, turned out to be linear, up to potential differences 4–6 V between the contacts (i.e., up to fields 40 V/cm).[2)] In the measurements of the photoconductivity we used only surface excitation and illuminated the entire area between the contacts. Under uniaxial compression conditions, the presence of contacts led to slight inhomogeneity of the deformation in the crystal; thus, the broadening of the free-exciton or exciton-impurity complex emission line, due to this inhomogeneity, does not exceed 0.1 MeV.

3. GAS–EHL PHASE DIAGRAM AND CRITICAL TEMPERATURE

In earlier investigations of EHL in silicon[17] we have established that the e-h density in the liquid phase in Si(1-2) is smaller by an approximate factor 7.5 than in the undeformed Si(2-6) crystal. So strong a decrease of the equilibrium density is due to the lifting of the degeneracy in the electron and hole bands by uniaxial deformation along the ⟨100⟩ direction. An equilibrium density in the EHL in Si(1-2) at $T=2$ K corresponds to $r_s=1.65$. Therefore the recombination-radiation spectrum of the EHL, as expected for such r_s, can still be adequately described within the framework of the e-h liquid.[18]

Figure 1 shows the emission spectra of Si(1-2) at a fixed density of pulsed excitation that produces $\bar{n}_{e,h}=(1.5\mp0.6)\cdot10^{17}$ cm^{-3}, measured at various temperatures and at zero delays of the strobing pulse. The spectra are superpositions of three bands: L, FE, and M, corresponding to emission of the EHL, of the free excitons, and of the excitonic molecules. With increasing temperature, the intensity of the L line decreases, and at $T>11$ K it can no longer be separated against the

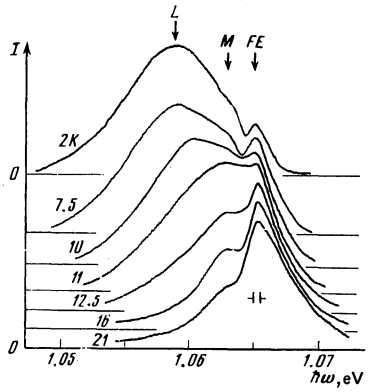

FIG. 1. Temperature behavior of the emission spectra of Si(1–2) under pulsed excitation ($\bar{n}\sim(1-2)\times10^{17}$ cm^{-3}). The spectra were recorded with a strobe of 0.15 μsec, delayed relative to the excitation pulse by 0.05 μsec.

background of the M line.

The temporal evolution of the emission spectra, measured at pulsed and surface excitations and at $T=7.5$ K, is shown in Fig. 2. The kinetics of the spectra in the interval $T=2$–10 K is qualitatively the same. The spectra show clearly the L, M, and FE lines, and the intensity of the FE and M lines changes little until the L line vanishes completely from the spectrum. The ratio of the damping times of the M line (τ_M) and of the FE line (τ_{FE}) does not depend on the temperature and amounts to $\tau_M/\tau_{FE}\sim0.55\mp0.05$. At $T=2$ K we have $\tau_{FE}=0.35$ μsec and $\tau_M=0.2$ μsec. These times become five times longer at $T=10$ K.

The described results find a natural explanation if it is assumed that up to $T\sim11$ K in a nonequilibrium e-h system with $\bar{n}\sim(1-2)\times10^{17}$ cm^{-3} stratification takes place into a gas phase (excitons and excitonic molecules) and a liquid phase.

The equilibrium density n_0 of the EHL is usually determined from an analysis of the form of the emission spectrum, which in the case of a metallic liquid is approximated by the expression[18]

$$I(h\nu)\sim\int_0^{h\nu}\frac{\varepsilon^{1/2}(h\nu-\varepsilon)^{1/2}\,d\varepsilon}{[1+\exp\{(\varepsilon-\varepsilon_F^{\,e})/kT\}][1+\exp\{(h\nu-\varepsilon-\varepsilon_F^{\,h})/kT\}]}, \tag{2}$$

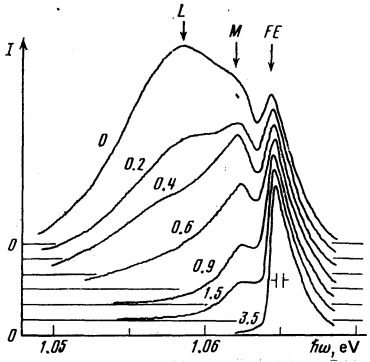

FIG. 2. Kinetics of the emission spectrum of Si(1–2) at $T=7.5$ K and under pulsed surface excitation ($\bar{n}\sim(1-2\times10^{17}$ cm^{-3}). The numbers on each of the spectrum indicate the delay time (in microseconds) of the strobe impulse of duration 0.15 μsec.

where $\varepsilon_F^{e,h}(n_0, T)$ is the Fermi energy of the electrons (holes). The energy of the photon emitted upon recombination is

$$\hbar\omega = h\nu + E_g - \varepsilon_{xc} - \hbar\Omega - n_0 \partial\varepsilon_{xc}/\partial n_0, \quad (3)$$

where E_g is the gap width, $\hbar\Omega$ is the energy of the emitted phonon, $h\nu$ is the energy reckoned from the red boundary of the spectrum, and $\varepsilon_{xc}(n_0)$ is the sum of the exchange and correlation energies. In our case, owing to the strong superposition of the L and M bands, it is impossible to use expression (2) directly for a determination of the density. However, as seen from the kinetics of the spectra on Fig. 2, the "red" region of the L band is free of overlap. Therefore, to determine n_0 at $T>4$ K we used expression (3) for the red boundary of the emission spectrum $\hbar\omega_R$ ($h\nu=0$), which is also uniquely connected with the density.[19] For a metallic EHL, the temperature dependences of the contributions made to the free energy per e-h pair from the exchange and from the correlation interactions cancel each other in the density and temperature regions of interest to us, where the plasma frequency is $\omega_p \gg kT/\hbar$ [in Si(1-2) we have $\hbar\omega_p/k > 150$ K at $\bar{n}_{e,h} > 10^{17}$ cm^{-3}]. Therefore at $T \lesssim 10$ K we can assume that $\varepsilon_{xc}(n_0, T) \approx \varepsilon_{xc}(n_0)$. Calculation of $\varepsilon_{xc}(n_0)$ for Si(1-2) was carried out in Ref. 19. The values of the equilibrium density n_0 obtained for $T=2$ from the position of $\hbar\omega_R$, using the results of this calculation as well as by approximating the form of the spectrum, agree within high accuracy.[17] We have therefore first constructed a calibration plot of $\hbar\omega_R(n_0)$, and then determined $n_0(T)$ from the experimental values of the red boundary of the spectrum. It turned out to be more convenient and more accurate to use the boundary values of the frequencies $\hbar\omega_{1/2}$ on the long-wave wing of the L band, where the intensity is half the intensity at the maximum. A correction was introduced here for the difference between $\hbar\omega_R$ and $\hbar\omega_{1/2}$, which in turn depends on n_0 and T in accord with (2). When the temperature is raised from 2 to 10 K, n_0 decreases from 4.5×10^{17} to $(3.6\pm0.2)\times10^{17}$ cm^{-3} or else r_s^0 increases from 1.65 to 1.76. On the whole the temperature dependence of the equilibrium density, up to $T\sim10$ K, is well described by the expression

$$n_0(T) = n_0(0)[1-\delta_n(kT)^2], \quad (4)$$

which, just as in Si(2-6),[5] is in complete agreement with the Landau theory for a quantum Fermi liquid. The experimental value $\delta_n = 0.21\pm0.3$ MeV^{-2} agrees well with the theoretically calculated[19] $\delta_n = 0.246$ MeV^{-2}.

We consider now the gas–EHL phase boundary, and disregard for the time being the question of the component ratio of the e-h gas (see Fig. 3). The gas-phase density n_g at which condensation set in was determined by threshold measurements of the intensity ratio of the lines L and FE as functions of $\bar{n}$. Near the condensation threshold $\bar{n} = n_g(T)$ the corresponding plot revealed a distinct break. The principal difficulty lay in the determination of the absolute values of the densities near the condensation threshold. To find the absolute values, calibration measurements of $\bar{n}$ were made at high excitation densities, when a plasma with $\bar{n} = 5\times10^{17}$ cm^{-3} was excited in the sample. It was assumed next that in the concentration region 3×10^{16}–5×10^{17} cm^3 the value

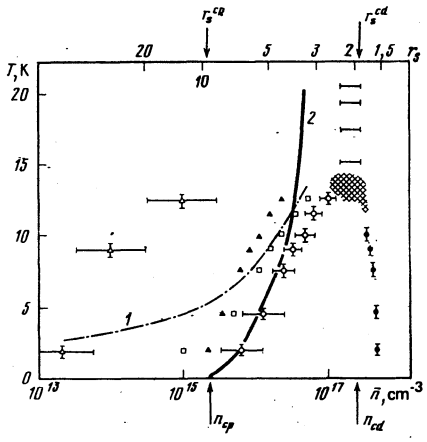

FIG. 3. Gas–EHL phase diagram in Si(1–2). ●—density of liquid phase, ○—density of saturated vapor of e-h gas, □—exciton density, ▲—excitonic-molecule density, Δ—density of free carriers. Curve 1—thermodynamic-equilibrium density of the exciton gas, curve 2—Mott-transition line. The critical region is shaded. At $T > T_c$, the horizontal segments show the region of the EP transition. The arrows indicate the values of the critical density of the EP transition, calculated in the approximations of the plasma (r_s^{cp}) and dielectric (r_s^{cd}) screenings.

of $\bar{n}$ is proportional to the excitation density. In this method no account was taken of the growth of the excitation region at large $\bar{n}$.[20] Thus, at $\bar{n} \geq 5\times10^{17}$ cm^{-3}, when the density of the e-h plasma can be independently estimated from the position of the red boundary of the spectrum $\hbar\omega_R$, we found that to increase n by a factor of 1.5 the pump density must be doubled. This effect, however, decreases rapidly with decreasing $\bar{n}$.[20] We emphasize that this method can only underestimate somewhat our values of n_g. The principal error in the estimated values of $\bar{n}$ is that the measurements are made under surface excitation conditions, when the density has inevitably a gradient in the interior of the sample.

The most reliable estimate of the density of the gas phase near the threshold at 2 K was obtained by an independent method under conditions of bulk excitation using a cw laser with $\lambda = 1.064$ μm. In this case, because of the known coefficient of absorption and the e-h pair lifetimes, n_g was estimated from the power density of the exciting light accurate to within a coefficient 2 ($n_g \approx 6\times10^{15}$ cm^{-3} at $T=2$ K). The obtained values of $n_g(T)$ are shown in Fig. 3.

To determine the critical temperature we investigated stratification into a gas and a liquid at $n=(1-2)\times10^{17}$ cm^{-3} and at various temperatures. This stratification manifests itself clearly in the recombination spectra up to temperatures $T \lesssim 10$ K (see Fig. 1). Variation of $\bar{n}$ at $T<T_c$ is accompanied by a change of only the ratio of the intensities between the L, FE, and M bands. The situation changes radically at $T>13$ K and $\bar{n} > 2\times10^{17}$ cm^{-3}. At these temperatures the spectra of the gas and liquid phases are no longer distinguishable, this being the main attribute of a critical region. At temperatures above critical, the increase of $\bar{n}$ by a factor 2–3 was accompanied only by a monotonic broadening of the resultant spectrum in the red direction.

The critical temperature in Si(1-2), estimated in this manner, turns out to be $T_c = 14 \mp 1.5$ K.

4. GAS OF EXCITONS, OF EXCITONIC MOLECULES, AND OF FREE CARRIERS NEAR THE CONDENSATION THRESHOLD AT $T = 2$K

The emission line of the free excitons predominates in the emission spectra of Si(1-2) at $T = 2$ K and $\bar{n}_{e,h} < 10^{15}$ cm^{-3}. At $\bar{n}_{e,h} > 10^{15}$ cm^{-3} a new band M appears in the spectra, besides the exciton band, and is attributed to the radiative decay of the excitonic molecules.[21] The properties of the form of the M band, its dependence on the temperature and on the pump,[15,22] and also the behavior in the magnetic field[23,24] confirm its molecular origin. At $T \sim 10$ K the band M remains in the spectra up to concentrations $n_g \sim 1.5 \times 10^{17}$ cm^{-3}. With increasing density in the gas phase, a danger arises that the spectral region of the M band can in principle receive contributions also from other radiation mechanisms, particularly those connected with exciton-exciton (electron) collisions, emission of exciton trions,[4] as well as that of e-h plasma. To monitor the possible contribution of these processes to the region of interest to us, we investigated the influence of the electric field (impact ionization) on the spectra, as well as the photoconductivity. These comprehensive investigations made it possible to determine the composition of the electron-hold gas along the gas–EHL phase boundary.

Figure 4 illustrates the action of impact ionization on weakly bound states in the spectral region corresponding to excitons and excitonic molecules. Figure 4a shows the spectra at $\bar{n} \sim 4 \times 10^{15}$ cm^{-3}. It is seen from the figure that the intensity of the M line decrease when an electric field $E \sim 10$ V/cm is turned on, and this line disappears completely from the spectrum in fields ~60 V/cm. In contrast, the free-exciton line in fields ~10 V/cm even increases somewhat, and at $E \sim 60$ V/cm it decreases only by a factor 1.5. Figure 4b shows the influence of the electric field on the M line and on the lines BE of excitons bound on boron atoms at $\bar{n} \sim 3 \times 10^{14}$ cm^{-3}, when the intensities of the BE and M lines in the absence of a field are comparable. It is seen that when an electric field is applied, the first to vanish is the M line. Thus, investigations carried out under impact-ionization conditions make it possible to exclude from consideration exciton-exciton collision processes, as well as to monitor the spectrum broadening due to the e-h plasma.

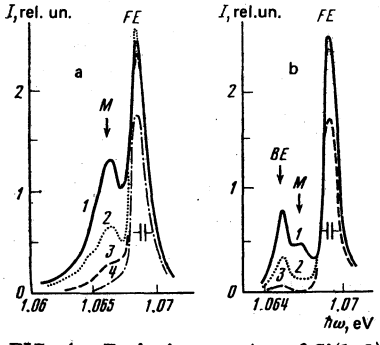

FIG. 4. Emission spectra of Si(1-2) at $T = 2$ K and at excitation densities 4×10^{15} cm^{-3} (a) and 3×10^{14} cm^{-3} (b). The spectra 1, 2, 3, and 4 were plotted for applied electric-field intensities 0, 20, 40, and 60 V/cm, respectively.

Under conditions when the M line appears in the spectra we have observed no singularities whatever in the dependence of the photoconductivity σ on the excitation density. In a wide range of e-h pair generation rate, $J \sim 10^{19}$–10^{22} cm^{-3} sec^{-1}, so long as the EHL line does not appear in the spectrum, we have $\sigma \sim \sqrt{J}$. At $\bar{n} \approx n_g \approx 5 \times 10^{15}$ cm^{-3} the value of σ reaches $5 \times 10^{-2} \Omega^{-1}$ cm^{-1}. The square-root dependence $\sigma \sim \sqrt{J}$ is typical of the case when the conductivity is due to the electrons and holes that did not have time to become bound into excitons. The concentration $n_{e,h}$ under stationary pumping is determined by the expression

$$n_{e,h} \approx (J/\gamma)^{1/2}, \tag{5}$$

where γ is the coefficient of finding into excitons. In silicon $\gamma \approx 10^3/T^2$ cm^3/sec.[25] At $\bar{n} = n_g$ an estimate of $n_{e,h}$ by Eq. (5) yields a value $\sim 2 \times 10^{13}$ cm^{-3}, which does not contradict the measured conductivity, inasmuch as in accordance with the known data the mobility of the electrons (holes) in Si at 2 K lies in the range from 10^4 to 10^5 cm^2/V-sec.[26] We note that to be able to attribute the M line to radiative recombination of trions we must assume that the concentration of the latter at $\bar{n} \sim 5 \times 10^{15}$ cm^{-3} must exceed 10^{15} cm^{-3}. This follows from the fact that at approximately identical radiative-recombination probability of the excitons and trions the integral intensity of the M line is larger than that of the FE line. Thus, investigations of the influence of the electric field on the emission spectra have confirmed that the M line is due to weakly bound state, and on the basis of a study of the photoconductivity it is possible to exclude the trions from consideration.

Knowing n_g, we can determine the absolute values of the concentrations of the excitons and of the excitonic molecules from the ratio I_{FE}/I_M of their integral intensities in the spectrum. The ratio of the probabilities of the radiative recombinations of the molecules and excitons, calculated using a variational wave function taken from Ref. 28, is 2.3.[3)] Substituting in the equations

$$n_{FE}/n_M = 2,3 I_{FE}/I_M, \qquad n_g = n_{FE} + 2n_M \tag{6}$$

the experimental values for n_g and I_{FE}/I_M, we find that at $T = 2$ K we have near the condensation threshold $n_{FE} = 1.3 \times 10^{15}$ cm^{-3} and $n_M = 2.4 \times 10^{15}$ cm^{-3} (see Fig. 3).

5. RATIO OF THE GAS PHASE COMPONENTS ALONG THE PHASE BOUNDARY. HIGH-TEMPERATURE REGION

It is seen from Fig. 3 that when the temperature rises in the range from 2 to 12 K the value of n_g increases from 6×10^{15} to 1.5×10^{17} cm^{-3} (r_s decreases from 7 to 2.7). The spectrum of the gas phase shows, up to temperatures $T \lesssim 12.5$ K, only two lines, FE and M, corresponding to the excitons and to the excitonic molecules. With increasing temperature, their average kinetic energy increases and the FE and M lines are broadened towards the violet side. The red edge of

the M line does not change with increasing temperature or with increasing excitation density at $\bar{n} \leqslant n_g$. The exciton emission line broadens only slightly at $\bar{n} > 5 \times 10^{16}$ cm^{-3}. Thus, there are no grounds for deducing from these observations that transformation of excitons into an e-h plasma takes place at densities $\bar{n} < n_g$ (at $T < 12.5$ K).

This conclusion is confirmed also by direct measurements of the kinetics of the photoconductivity, which was investigated simultaneously with the kinetics of the emission of the FE and M lines (see Fig. 5). In the measurement of the photoconductivity, the entire region between the contacts was excited and the maximum density of the e-h pairs under pulse excitation was (1–2) $\times 10^{17}$ cm^{-3}. It is seen from Fig. 5 that the conductivity σ is high only during the first 0.15 μsec after the excitation pulse. At delays $\tau_d \sim 0.2$ μsec, σ decreases by one order of magnitude, after which it changes much more slowly. With decreasing excitation density, the photoconductivity peak shortens in time simultaneously with the decrease of σ_{max}. It is quite natural to attribute this photoconductivity peak to formation of an e-h plasma of high density ($>10^{17}$ cm^{-3}) in the crystal after the pulse, while the abrupt decrease of σ at $\tau_d > 0.1$ μsec can be attributed to the rapid decrease of the number of free electrons and holes due to their binding into excitons. Unfortunately, we did not have a time resolution better than 0.1 μsec, and were not able for the time being to trace the time evolution of the emission spectrum with delays $\tau_d < 0.1$ μsec. In the spectra recorded with a 0.1-μsec strobe, only some decrease of the intensity near the red edge is observed when τ_d is increased from 0 to 0.2 μsec. The total intensity of the radiation increases somewhat in this case (σ decreases by one order of magnitude). At delays $\tau_d \approx 0.2$ μsec, the M and FE lines take on their "standard" form. It is seen from Fig. 5 that when I_M is decreased by more than one order of magnitude, i.e., practically up to the vanishing of the M line from the emission spectrum, σ decreases to less than one-half. At lower temperatures, $T = 7.5$–10 K, the weakening of the time dependence of σ takes place also before the vanishing of the EHL emission line, since the EHL drops make no contribution to the electric conductivity since they are electrically neutral over all.

The absolute concentrations of the excitons and molecules in the gas phase, just as at $T = 2$ K, were obtained with the aid of relations (6) (Fig. 3). The obtained density of the saturated vapor of the exciton gas can be compared with the thermodynamic-equilibrium density (see curve 1 in Fig. 3) estimated from the formula

$$n_{FE} = \left(\frac{m_{FE} kT}{2\pi\hbar^2}\right)^{3/2} g_{FE} \exp\left(-\frac{\varphi}{kT}\right), \tag{7}$$

where $m_{FE} = 0.6 m_e$ and $g_{FE} = 8$ are respectively the translational mass and the statistical weight of the exciton, φ is the EHL binding energy, and m_e is the mass of the free electron. It is seen from Fig. 3 that the equilibrium between the exciton gas and the EHL sets in only at sufficiently high temperatures, $T \gtrsim 7$ K. The same situation obtains also in undeformed silicon.[5] These deviations from detailed balancing in the low-temperature part of the phase boundary are due to a considerable degree, apparently, to overheating of the EHL drops by the intense nonradiative recombination of the e-h pairs.

At the same time, thermodynamic equilibrium manages to set in between the excitons and the excitonic molecules in the gas phase. In particular, this is confirmed by the fact that along the gas–EHL phase boundary the ratio of the lifetimes of the excitons and of the excitonic molecules remains constant, with high accuracy, at $\tau_M/\tau_{FE} \sim 0.55$. Under equilibrium conditions, the concentrations n_{FE} and n_M are connected by the Saha equation[29]

$$n_M = n_{FE}^2 \left(\frac{2\pi m_M \hbar^2}{kT m_{FE}^2}\right)^{3/2} \frac{g_M}{g_{FE}^2} \exp\left(\frac{\Delta}{kT}\right), \tag{8}$$

where Δ is the binding energy of the excitonic molecule, $m_M = 2m_{FE}$, and the statistical weight is $g_M = 6$. Actually, along the entire gas-liquid coexistence curve the ratio n_M/n_{FE}^2 is well described by Eq. (8) if it is assumed that Δ is limited to 0.55 ± 0.2 MeV. This value agrees well with the $\Delta = 0.55 \pm 0.15$ MeV obtained by us earlier from the temperature dependence of the ratio n_M/n_{FE}^2 at $T \lesssim 4$ K.[17] We note also that at $T \gtrsim 10$ K, owing to the smallness of Δ compared with kT, the ratio of the concentrations n_{FE} and n_M is determined mainly by the pre-exponential factor.

In addition to the excitons and biexcitons, the gas phase contains also free electrons and holes. Although no direct measurements of the mobilities $\mu_{e,h}$ were made by us, we can estimate the order of magnitude of n_e from measurements of the photoconductivity σ. The function $\sigma(I_{FE})$ under pulsed excitations and at long delay times $\tau_d > 5$ sec, when $\bar{n} \approx n_{FE} \lesssim 10^{15}$ cm^{-2}, takes the square-root form $\sigma \sim \sqrt{I_{FE}}$. At such small $\bar{n}$, the mobility is independent of the gas density and $\sigma \sim n_e$. The $\sigma \sim \sqrt{I_{FE}} \sim \sqrt{n_{FE}}$ dependence agrees with the Saha relation between the excitons and the free carriers under thermodynamic equilibrium:

$$n_{FE} = n_e^2 \left(\frac{2\pi\hbar^2}{kT} \frac{m_{FE}}{m_e m_h}\right)^{3/2} \frac{g_{FE}}{g_e g_h} \exp\left(\frac{\mathrm{Ry} - \Delta\varepsilon}{kT}\right), \tag{9}$$

where $g_{e,h}$ are the multiplicities of the degeneracy of the electrons (holes) [$g_e = 4$, $g_h = 2$, $g_{FE} = 8$ in Si(1-2)]. $\Delta\varepsilon$ is the correction that must be added to the binding energy to account for screening of the Coulomb interaction, and can be neglected at small $\bar{n}$.

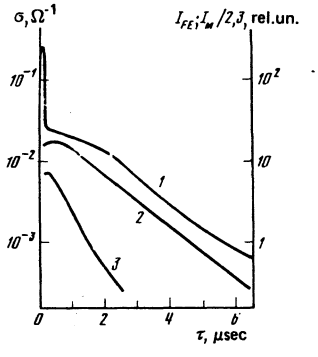

FIG. 5. Kinetics of the photoconductivity σ (curve 1) and of the emission-line intensities of the excitons (curve 2) and of the excitonic molecules (curve 3) at 12.5 K and $\bar{n} \sim 2 \times 10^{17}$ cm^{-3}.

From (9) we easily find that at $n_{FE}=10^{15}$ cm^{-3} and $T=12.5$ K we have $n_e=10^{13}$ cm^{-3}. We note that at this value of n_e we obtain for the mobility $\mu_e=\sigma/n_e e$ the value 6×10^4 cm^2/V-sec, which agrees in order of magnitude with the published data.[26] At $n>10^{15}$ cm^{-3} ($\tau<5$ μsec), σ increases with increasing I_{FE} more rapidly than in accord with a square-root law (Fig. 5). At such $\bar{n}$ this can be reconciled with the expected decrease of the exciton binding energy on account of screening of the Coulomb interaction by the free carriers. At low densities n_e we have[29]

$$\Delta\varepsilon\approx\frac{8\pi n_e e^2}{\varkappa kT}\cdot 2a_B, \tag{10}$$

where $\varkappa$ is the dielectric constant. Some weakening of the $\sigma(I_{FE})$ dependence at $\tau_d<2$ μsec (Fig. 5) is apparently due to the decrease of the mobility at large concentrations of the e-h pairs ($r_s\sim5$–2.5). A considerable decrease of μ at such r_s was observed earlier in Ge (Ref. 27) in an investigation of $\mu(\bar{n})$ in a wide range of temperatures. If it is assumed that in Si, just as in Ge, the change of μ with increasing $\bar{n}$ in this region of r_s does not exceed an order of magnitude, then we get from measurements of the conductivity a value 10^{15} cm^{-3} for the density n_e at $T=12.5$ K and at $\bar{n}=n_g=10^{17}$ cm^{-3}. Similar estimates for n_e at $\bar{n}=n_g$ and $T=9$ K lead to $n_e\approx10^{14}$ cm^{-3}. The value of $\Delta\varepsilon$ calculated in accord with Eq. (10) is in this case $\sim(1/3$–$2/3)$ Ry. We note, however, that at such high densities the expression (10) overestimates the value of $\Delta\varepsilon$.[29]

6. EXCITON-PLASMA TRANSITION AT $T>T_c$

The transformation of the emission spectrum of the excitons in an e-h plasma was investigated at higher pumps and temperatures $T\gtrsim T_c$. Figure 6 shows the kinetics of the emission spectrum at $T=21$ K under pulsed pumping with $\bar{n}=4\times10^{17}$ cm^{-3}. During the first 0.15 μsec of the excitation pulse the spectrum is a broad structureless band covering the region in which the M and FE lines are located. When the pulsed pump is increased, $\bar{n}>4\times10^{17}$ cm^{-3}, the width of the band increases mainly on account of its red wing. With increasing delay, this band becomes somewhat narrower and its red boundary shifts towards higher energies. The forms of the spectrum of the broad structureless band in the temperature interval 13–21 K and under pulsed pumping with $n=4\times10^{17}$ cm^{-3} have approximately the same kinetics. At delays $\tau_d\sim0.3$–0.5 sec, when the average density decreases to $\bar{n}\lesssim1.5\times10^{17}$ cm^{-3}, the FE and M line begin to manifest themselves distinctly in the spectrum. At 21 K the "red" wing of the M line retains its form when the ratio I_M/I_{FE} is decreased by approximately a factor of 2. At $T<20$ K the form of the red edge of this line remains constant in a larger range of variation of the ratio I_M/I_{FE}. At $T>22$ K the form of the emission spectrum in the region of the M line changes all the time.

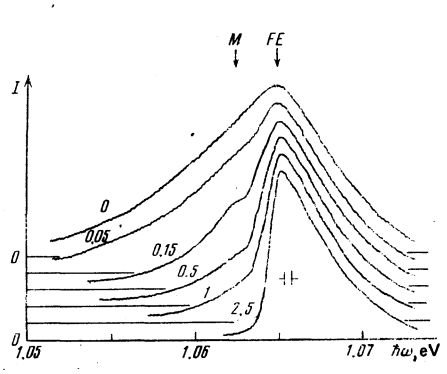

FIG. 6. Kinetics of the emission spectrum of Si(1-2) at $T=21$ K and under pulsed surface excitation ($\bar{n}\sim4\times10^{17}$ cm^{-3}). The numbers on the spectra indicate strobe-pulse delay times. The duration of the strobing pulse is 0.1 μsec.

The smearing of the discrete spectral structure corresponding to the excitons and excitonic molecules (the FE and M bands) is most likely due to the EP transition. Our estimate of the critical density n_c for the EP transition at $T=13$–21 K yields $n_c=(1.5$–$3)\times10^{17}$ cm^{-3} ($r_s^c=2$–2.5). Thus, the EP transition takes place in Si(1-2) near the critical region (see Fig. 3). It is possible to observe the EP transition in Si(1-2) at temperatures lower (by an approximate factor of 2) than in Si(2-6),[5] because of the substantially higher densities that are realized in the gas phase in these crystals. We recall that within the framework of the model of plasma screening of the Coulomb interaction we expected the ionization disintegration of the excitons to take place jumpwise and to be possibly accompanied by stratification of the excited volume into regions occupied by strongly and weakly ionized exciton gas.[14-16] In Si(1-2), however, just as in Si(2-6), the transformation of the discrete exciton spectrum into a plasma spectrum is more likely of the smooth (diffuse) type. At $T\gtrsim25$ K in the vicinity of the EP transition, the conductivity also changes smoothly. With decreasing temperature, a faster increase of the conductivity is observed in this region. However, even at $T=15$ K the increase of the conductivity is smaller by approximately one order of magnitude than that expected under conditions of total ionization of the excitons. This behavior of the conductivity is apparently due to the strong e-h correlations in the vicinity of the EP transition (at $r_s\sim2.5$–2).

7. CONCLUSION

Our analysis of the composition of the nonequilibrium e-h gas along the gas–EHL phase boundary has established that in Si(1-2) the excitonic states retain their individuality up to densities corresponding to the dimensionless parameter $r_s\sim2.5$. It is of interest to compare these experimental observations with the existing estimates of the EP transition. According to the Mott criterion [Eq. (1)], which uses the approximation of the plasma screening of the Coulomb interaction, the critical density n_{cp} for Si(1-2) at $T=0$ K corresponds to $r_s^{cp}\approx10$ (shown by the arrow in Fig. 3). It is seen that as $T\to0$ this critical density turns out to be directly in the two-phase region, i.e., the EP transition is preceded by condensation into EHL. With increasing temperature the effectiveness of the screening decreases and the critical values n_{cp} shift towards higher densities. It is easy to calculate the line of the Mott transition for

Si(1-2) in the entire range of temperatures of interest to us (2–15 K), using for this purpose the following expression for the static screening radius:

$$r_0^{-2}=\sum_{e,h}\frac{e^2(m_{e,h}^*)^{1/2}(2kT)^{1/2}}{\varkappa\pi\hbar^3}F_{-1/2}\left(\frac{\varepsilon_{e,h}^F}{kT}\right), \qquad (11)$$

which is valid for an arbitrary degree of degeneracy of the electron and hole gases. In Eq. (11), $F_{-1/2}(\varepsilon_{e,h}^F/kT$ is the Fermi integral. We note that allowance for the dynamic screening effect, as shown recently in Ref. 10, hardly changes the final result. It turned out (see Fig. 3) that in the temperature interval 2–8 K we have $n_g \approx n_{cp}$, and at $T>8$ K the threshold density of the $e-h$ gas, which consists mainly of excitons and excitonic molecules, exceeds noticeably the critical density of the EP transition ($n_g > n_{cp}$) calculated in accordance with the Mott criterion. This means that the plasma-screening approximation is too crude and does not describe the states of the $e-h$ gas in this region. In our opinion this is not surprising, since the values of the critical density obtained on the basis of this approximation turn out to be in the region where the $e-h$ gas cannot be regarded as weakly interacting. It is natural to expect that at such densities and temperatures the state of the $e-h$ gas should be noticeably influenced by the $e-h$ correlations, which are not taken into account within the plasma-screening approach. In this connection, great interest attaches to estimates recently obtained for the critical density[11] in the approximation of the dielectric screening of the Coulomb interaction. It was found in these estimates that the dielectric gap in the spectrum of the single-particle excitations of an assembly of excitons with high density becomes vanishedly small at values $r_s^{cd} \approx 1.8$, which comes close to our experimental values. It should be noted in this connection that in semiconductors with a direct gap the discrete structure of the excitonic spectrum becomes smeared out and practically vanishes at densities corresponding to $r_s \sim 2$.[30,31]

We call attention, in conclusion, to the fact that the kinetic properties of the free electrons and holes in the vicinity of the EP transition are presently less investigated and less understood. In this density and temperature region, the carrier motion correlates strongly with the Coulomb interaction, which is not completely screened. Therefore the mobility and the resultant conductivity of the carriers in this transition exciton-plasma region is apparently greatly modified by the strong $e-h$ correlations. An investigation of this question is of independent interest.

The authors thank L. V. Keldysh, Ya. E. Pokrovskiĭ, and A. P. Silin for helpful discussions.

[1)]Approximately the same result was recently obtained in Ref. 10, where account was taken of effects of dynamic screening of the Coulomb interaction.

[2)]The authors are deeply grateful to S. I. Shevchenko for the opportunity of preparing the ohmic electric contacts by this method.

[3)] The authors thank V. M. Édel'shteĭn for calculating the ratio of the radiative decay probabilities of the excitonic molecules and of the excitons.

[1]L. V. Keldysh, Proc. 9th Internat. Conf. on Semiconductor Physics, Moscow, 1968, p. 1308. Éksitony v poluprovodnikakh (Excitons in Semiconductors), Nauka, 1971, p. 5.
[2]Y. E. Pokrovskii, Phys. Status Solidi A **11**, 385 (1972).
[3]G. A. Thomas, T. M. Rice, and J. C. Hensel, Proc. Intern. Conf. Phys. Semicond., XII, Stuttgart, Teubner, 1974, p. 105.
[4]G. A. Thomas, J. B. Mock, and M. Capizzi, Phys. Rev. B **18**, 4250 (1979).
[5]A. F. Dite, V. D. Kulakovskiĭ, and V. B. Timofeev, Zh. Eksp. Teor. Fiz. **72**, 1156 (1977) [Sov. Phys. JETP **45**, 604 (1977)].
[6]J. Shah, M. Combescot, and A. H. Dayem, Phys. Rev. Lett. **38**, 1497 (1977).
[7]V. S. Bagaev, T. I. Galkina, O. V. Gogolin, and L. V. Keldysh, Pis'ma Zh. Eksp. Teor. Fiz. **10**, 309 (1969) [JETP Lett. **10**, 195 (1969)].
[8]M. A. Lampert, Phys. Rev. Lett. **1**, 450 (1958).
[9]F. I. Rogers, H. C. Graboske, and D. J. Harwood, Phys. Rev. A **1**, 1577 (1970).
[10]R. Zimmermann, K. Kilimann, W. D. Kraeft, D. Kremp, and G. Röpke, Phys. Status Solidi B **90**, 175 (1978).
[11]V. E. Bisti and A. P. Silin, Fiz. Tverd. Tela (Leningrad) **20**, 1850 (1978) [Sov. Phys. Solid State **20**, 1068 (1978)].
[12]N. F. Mott, Adv. Phys. **16**, 49 (1967); Metal-Insulator Transitions, Barnes and Noble, N.Y., 1974.
[13]P. L. Hugon and A. Ghazali, Phys. Rev. B **14**, 602 (1976).
[14]Z. A. Insepov and G. E. Norman, Zh. Eksp. Teor. Fiz. **62**, 2290 (1972) [Sov. Phys. JETP **35**, 1198 (1972)]. Z. A. Insepov, G. E. Norman, and L. Shchurova, Zh. Eksp. Teor. Phys. **71**, 1960 (1976) [Sov. Phys. JETP **44**, 1028 (1976)].
[15]W. Ebeling, W. Kraeft, and D. Kremp, Ergebnisse der Plasmaphysik und der Gaselektronik, Vol. 5, ed. by R. Kompe and M. Steenbeck, Akademie-Verlag, Berlin, 1976.
[16]T. M. Rice, Proc. Intern. Conf. Phys. Semicond., XII, Stuttgart, Teubner, 1974, p. 23.
[17]V. D. Kulakovskiĭ, V. B. Timofeev, and V. M. Édel'shteĭn, Zh. Eksp. Teor. Fiz. **74**, 372 (1978) [Sov. Phys. JETP **47**, 193 (1978)].
[18]J. C. Hensel, T. G. Phillips, and G. A. Thomas, Solid State Phys. **32**, 323 (1977).
[19]P. Vashishta, J. P. Bhattacharyya, and K. S. Singwi, Phys. Rev. B **10**, 5108 (1974).
[20]V. S. Bagaev, L. V. Keldysh, N. N. Sibel'din, and V. A. Tsvetkov, Zh. Eksp. Teor. Fiz. **70**, 702 (1976) [Sov. Phys. JETP **43**, 362 (1976)].
[21]V. D. Kulakovskiĭ and V. B. Timofeev, Pis'ma Zh. Eksp. Teor. Fiz. **25**, 487 (1977) [JETP Lett. **25**, 458 (1977)].
[22]P. L. Gourley and J. P. Wolfe, Phys. Rev. Lett. **40**, 526 (1978).
[23]V. D. Kulakovskiĭ, A. V. Malyavkin, and V. B. Timofeev, Zh. Eksp. Teor. Fiz. **77**, 752 (1979) [Sov. Phys. JETP **50**, 380 (1979)].
[24]V. M. Édel'shteĭn, Zh. Eksp. Teor. Fiz. **77**, 760 (1979) [Sov. Phys. JETP **50**, 384 (1979)].
[25]J. Barran, M. Hekman, and M. Broussean, J. Phys. Chem. Solids **34**, 381 (1973).
[26]V. A. Grazhulis, V. Yu. Mukhina, Yu. A. Osip'yan, and S. A. Shevchenko, Zh. Eksp. Teor. Fiz. **68**, 2149 (1975) [Sov. Phys. JETP **41**, 1076 (1975)].
[27]M. Glicksman, M. N. Gurnee, and J. R. Meyer, Proc. Oji Seminar at Tomakomai, Japan, Springer-Verlag, Berlin, N.Y., 1976, p. 219.
[28]W. F. Brinkman, T. M. Rice, and B. Bell, Phys. Rev. B **8**, 1570 (1973).
[29]T. M. Rice, Solid State Phys. **32**, 1 (1977).
[30]V. G. Lysenko and V. I. Revenko, Fiz. Tverd. Tela (Leningrad) **20**, 2144 (1978) [Sov. Phys. Solid State **20**, 1238 (1978)].
[31]A. Frova, P. Schmid, A. Grisel, and F. Levy, Solid State Commun. **23**, 45 (1977).

Translated by J. G. Adashko